CDF/ANAL/JET/CDFR/10841
Draft 0.2
September 2, 2012

Central Exclusive Production of Hadrons (Double Pomeron Exchange) in CDF Public Note

Artur Swiech, Maria Zurek
Jagiellonian University, Cracow, Poland

Michael Albrow, Jonathan Lewis
Fermi National Accelerator Laboratory, USA

Denys Lontkowsky, Inna Makarenko
Univ. of Kiev, Ukraine

Abstract

We present a study in CDF of $p\bar{p}$ collisions at the Tevatron that have 2 charged hadrons in the central region, $|\eta| < 1.3$ with large rapidity gaps (no hadrons) on either side. The reaction is $p+\bar{p} \to p+X+\bar{p}$, where the "+" stands for a rapidity gap G; we use the notation GXG. The studied final state is often the result of the decay of a single neutral resonance, such as f_0^0 or f_2^0 states. These events are expected to be dominated by double pomeron, $\mathbb{P}$, exchange in the t-channel; hence $\mathbb{P}+\mathbb{P} \to X$. Only specific quantum numbers for X are allowed.

We use data taken at $\sqrt{s} = 1960$ GeV and 900 GeV.

This data provides a useful window on hadron spectroscopy, as well as providing benchmarks for testing pomeron models.

1 Introduction

The pomeron, $\mathbb{P}$, can be defined as the carrier of 4-momentum between protons when they scatter elastically at high (i.e. collider) energies. It is therefore a strongly interacting color singlet state, at leading order a pair of gluons: $\mathbb{P} = gg$. In QCD it cannot be a pure state, quark pairs and other gluons must evolve in when Q^2, which we can equate with the 4-momentum transfer^2 t, becomes large. When Q^2 is small ($\lesssim$ 2 GeV^2) which is usually the case with pomeron exchange, perturbative QCD cannot be used to calculate cross sections, as the coupling $\alpha_s(Q^2)$ becomes of order 1.

Non-perturbative methods, such as Regge theory, are more applicable [3, 2, 1]. It is a challenge to theorists to derive Regge theory from QCD, but after 40 years it has not happened. Meanwhile the subject is largely data-driven and phenomenological, hence the value of new data such as in this study.

It is known that one can have pp interactions with more than one pomeron, $\mathbb{P}$, exchanged, known as double pomeron exchange, D$\mathbb{P}$E. See [4] for a recent review. This process $\mathbb{P}+\mathbb{P} \to X$ allows an experimental approach to better understand the pomeron. One should not think of the pomerons as isolated entities being emitted from the protons that then interact; the pomeron is only a t-channel exchange. D$\mathbb{P}$E can also be thought of as $g + g \to X$ with another (soft) gluon(s) exchanged to cancel the color and allow the protons to (sometimes) emerge intact. Sometimes the protons will dissociate into a low-mass state, e.g. $p \to p\pi^+\pi^-$. This is diffractive dissociation; it should not affect the properties of X. In CDF we cannot detect the outgoing protons, but it does not matter for this study as long as we can select events with large rapidity gaps $\Delta y \gtrsim 4$ on each side of X. However the cross sections we measure will be larger than the fully exclusive process: $p + X + p$.

When $M(X) \lesssim 4$ GeV/c^2 the interest is for specific ("exclusive") states with well defined quantum numbers; when $M(X) \gtrsim 10$ GeV/c^2 the (multi-)partonic structure of the pomeron is probed, and one may find new phenomena related to the fact that it is *not* a hadron, but is nevertheless a strongly-interacting color singlet without valence quarks. High mass central states are the subject of a different study.

Understanding these interactions will enhance our understanding of nonperturbative QCD. CDF is an excellent detector for this physics, and while the LHC detectors would be suitable, the running conditions are currently such that there are very few interactions with no pile-up, which is a necessary condition for this physics (unless one measures both leading protons, as in the FP420 projects). We also have data at both $\sqrt{s} = 900$ GeV and 1960 GeV, and the s-dependence is instructive as we shall show.

2 Relevant CDF detectors

For the results in this study we used all the CDF detectors with the exception of the time-of-flight system. The muon chambers are used only for background rejection, and the silicon detectors for track quality enhancement. We will select events with just 2 COT (Central-Outer-Tracker) tracks, with $\sum Q = 0$. We want to select events with no other hadrons produced, and will require that all the calorimetry (except around the impact points of the charged particles), the BSC-1 (Beam-Shower-Counters-1), and the CLC (Cherenkov-Luminosity-Counters) have signals consistent with noise. This data was taken after the outer BSC counters (BSC-2 and BSC-3) and the MiniPlug were decommissioned. We are therefore blind to $|\eta| > 5.9$ and accept events where the proton was quasi-elastically scattered ("el") or where it fragmented into a low mass state ("inel"). There will be three classes: el+el, el+inel, and inel+inel.

2.1 Forward detectors for gap requirements

We put BSC-1, which covers $5.4 < |\eta| < 5.9$, in veto in the level 1 trigger. The CLC were also put in veto. The CLC cover $3.75 < |\eta| < 4.75$ on each side. BSC-1 and the CLC together cover range from $|\eta| = 3.75$ to 5.9, and $\Delta\eta = 2.15$ is not enough for pomeron dominance (Reggeon exchanges are still important). We therefore extend the veto region using the forward plug calorimeter, which covers $2.11 < |\eta| < 3.64$, at level 2 trigger. The small "hole" between 3.64 and 3.75 is not very important, partly because of the "splash-out" detection by the CLC, and also because the chance of having no particles between 2.11 and 5.9 *except* in that hole is small, and will give a small background. There is also a gap between the CLC and BSC1, $\eta = 4.75$ - 5.4. We were able to show that the probability that an event satisfying the forward plug, CLC and BSC1 vetos, and therefore our trigger, has a hit in the small uncovered gap is only a few %, by simulating the trigger in 0-bias data taken when the Miniplugs were operational. Off-line we will require that the gaps extend through the plug regions to $|\eta| = 1.3$, so apart from the small cracks we have gaps $\Delta\eta > 4.6$.

3 Rapidity gap cuts, exclusive selection

To understand the noise levels in all the detectors, we use zero-bias (bunch crossing) triggers, taken during the same periods. We did this independently for the 1960 GeV and 900 GeV runs. We divided the 0-bias data into two classes:

- (A) No interactions, defined as no tracks, no muon stubs, and no CLC hits,
- (B) all the other events, totally dominated by one or more inelastic interactions.

For each subdetector we compare the signals in the two classes, with (A) dominated by noise.

Fig. 1 shows the distribution of the sum of the ADC counts or Energy in different parts of CDF detector ($\log_{10}$ scale) showing the noise-dominated and signal-dominated distributions. The interaction data shows a component at the noise level, because of course a sizeable fraction of interaction events have a gap in part of the detector.

We require that the central detectors are at the noise level, except for the two charged tracks. The tracks are extrapolated to the calorimeters, and allowing for any energy in a cone of radius $\sqrt{\Delta\eta^2 + \Delta\phi^2} < 0.3$ around the impact points we apply the same procedure as for the forward detectors.

4 Exclusive efficiency and effective luminosity

As any cross sections that we measure use data with no other inelastic collision to spoil the exclusivity (no pile-up), we need to know the probability of having no pile-up. This is the *exclusive efficiency* $\varepsilon(excl)$. To calculate it, we look at 0-bias data, for which the

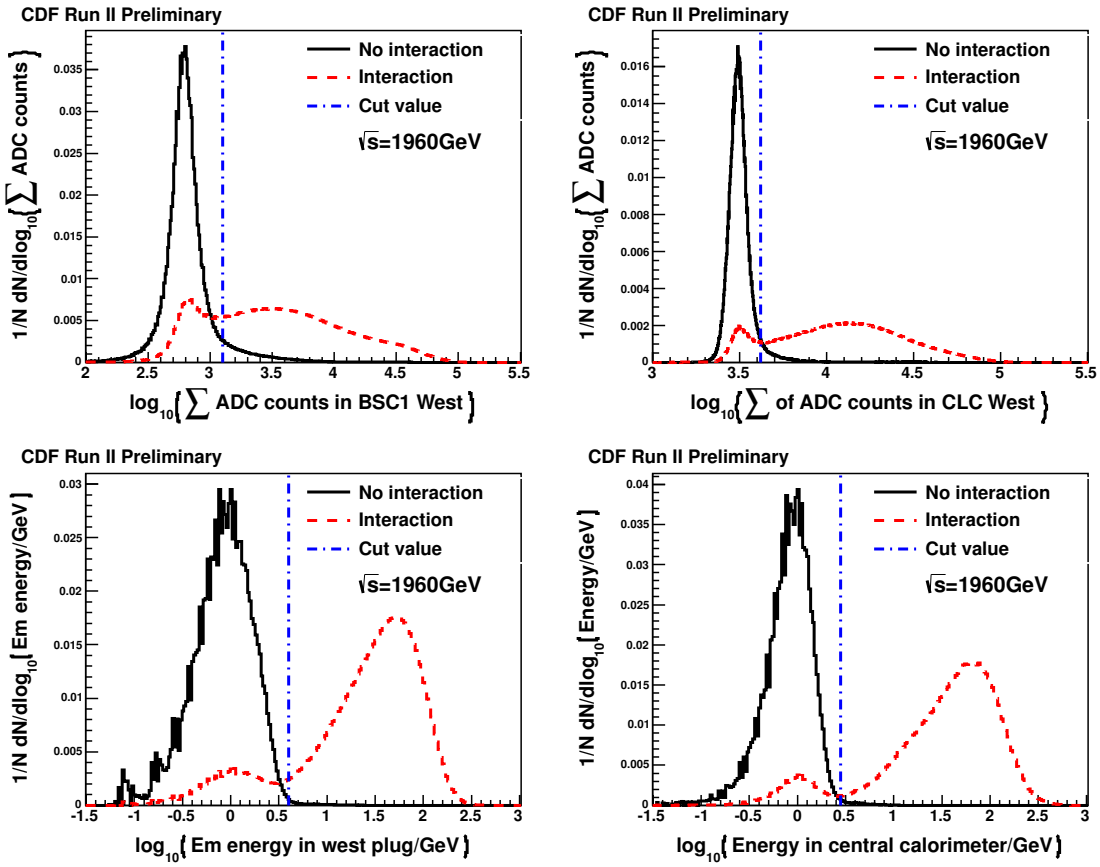

Figure 1: Interaction - No interaction separation in BSC-1 West, CLC West, Forward Plug West and Central calorimeter determined for Zero-Bias data taken from same period as triggered data for $\sqrt{s} = 1960$ GeV. Blue lines indicate cut value.

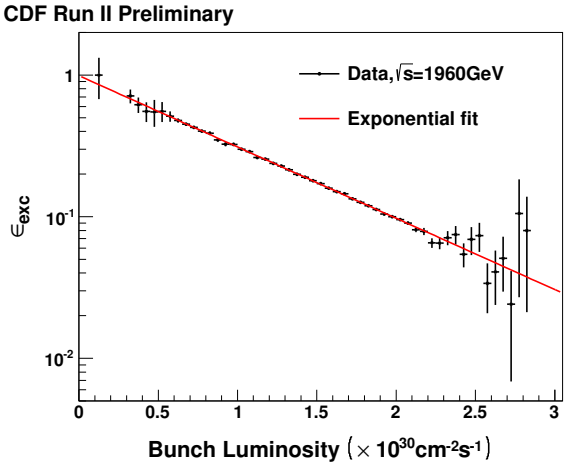

Figure 2: Exclusive efficiency as a function of bunch luminosity for $\sqrt{s} = 1960GeV$. Red line shows the exponential fit.

luminosity of the particular bunch crossing, L_{bunch}, is recorded. Applying all the same cuts as before, we measure, as a function of L_{bunch}, the probability $P(0)$ that all the detectors are in the noise, so apparently there was no inelastic collision (except low mass diffraction with very forward fragmentation products). The average number of such inelastic collisions is $\bar{n} = \mu = L_{bunch} \times \sigma_{inel-vis}/f_X$, where f_X is the orbital frequency of the Tevatron (i.e. the number of times per second a particular bunch passes, which is 46.5/s). As the actual number follows a Poisson distribution, $P(0) = e^{-\mu}$. This is plotted for the two energies in Figs. 2 and 3, together with an exponential fit. The fit should extrapolate to 1.0 at $L_{bunch} = 0$, and it is very close, meaning that there is almost no noise above the cuts that would give a non-empty detector even with no luminosity. The slope (if the bunch luminosity is known) in principle gives $\sigma_{inel-vis}$, or rather the cross section for producing any hadrons in $-5.9 < \eta < +5.9$, which does not include low mass diffraction.

We see that the distributions, labelled $\varepsilon(excl) = P(0)$ in the figures, are good exponentials except at the highest 900 GeV bunch luminosities, where there are very few events. The exponential fits, give $\sigma_{inel-vis} = 53.9$ mb at 1960 GeV and $\sigma_{inel-vis} = 62.8$ mb at 900 GeV.

5 Two exclusive tracks; track quality cuts

The selection of 2-track events is made with a sequence of cuts. We give higher priority to having a clean, well measured, sample than to efficiency. We use the higher statistics 1960 GeV data to define the track cuts, and apply the same cuts at 900 GeV. We define the central region (i.e. region for reconstructed tracks) to be in $|\eta| < 1.3$, where the trigger was active. The opening angle cut, as well as the requirement of zero muons, reduce the small background from cosmic ray tracks with $\theta_{3D} = \pi$. The track quality

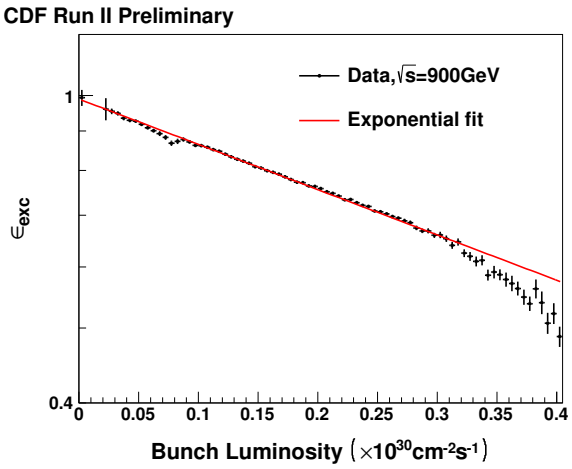

Figure 3: Exclusive efficiency as a function of bunch luminosity for $\sqrt{s} = 900GeV$. Red line shows the exponential fit.

cuts consists of:

- Impact parameter to the nominal beam line cut, $d_0 < 0.1$ mm,
- The difference in z projected to the beam line $|dz_0| < 1.0$ cm,
- The number of COT hits in axial layers $\geqq 25$,
- The number of COT hits in stereo layers $\geqq 25$,
- $\chi^2/\mathrm{DoF} < 2.5$,

To have a well-defined fiducial region and avoid poorly known thresholds we require both tracks to have $p_T > 0.4$ GeV/c. Additionally to be able to calculate the proper acceptance, we require the rapidity of the two track state to be $|y| < 1.0$. Finally we require the tracks to have opposite charge. The numbers of (++) and (- -) pairs are similar with a few more (++) events. The excess (++) probably comes from spallation, beam gas etc. The number of events in (- -) may be used to estimate the non-exclusive background contamination in our events.

5.1 Mass distributions, resonance structures, and kinematic properties

We now present mass spectra uncorrected for acceptance. This data may make a valuable contribution to meson spectroscopy. States with a large gluonic content ("glueballs" or hybrids) should be favored, in contrast to $\gamma\gamma \to X$ where $q\bar{q}$ stated are favored.

Fig. 4 and Fig. 5 show the mass distributions of the events for all p_T, with statistical errors only. We have not used any particle identification, and assume here that h^+h^-

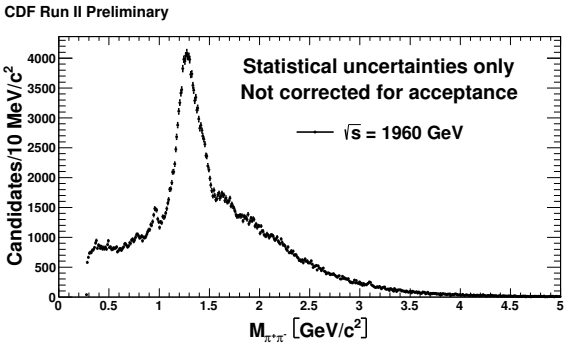

Figure 4: Invariant mass distribution of 2 particles assuming pion mass - not corrected for acceptance. $\sqrt{s} = 1960$ GeV

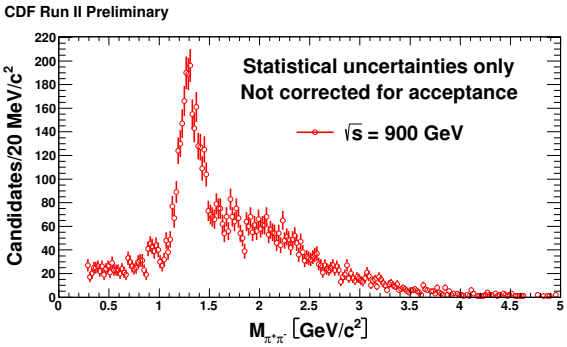

Figure 5: Invariant mass distribution of 2 particles assuming pion mass - not corrected for acceptance. $\sqrt{s} = 900$ GeV

is $\pi^+\pi^-$. This was found to be a good approximation in DIPE at the CERN ISR. Later in this note we discuss the K^+K^- "contamination" in this plot, and show that it must be small.

The basic features are similar, but in detail the ratio of the two distributions depends on the mass, although the acceptances should be simillar at both energies. The peak at 980 MeV is the $f_0(980)$ state. We see weak signs of the $\rho(770)$, width = 150 MeV, which can be produced by exclusive photoproduction ($\gamma + \mathbb{P}$) but not in DIPE (it has CP = -1,-1). The sharp drop at 1 GeV/c^2, on the high side of the $f_0(980)$, occurs just at the K^+K^- threshold. J.Rosner has argued [5] that when a new channel opens up it causes a "cusp" in the existing scattering amplitudes. The dominant peak between 1.1 GeV and 1.6 GeV is not well fit by a single state (either Gaussian or Breit-Wigner) but is fit by two states, consistent with the $f_2(1270)$ and the broad $f_0(1370)$. Strictly speaking, one should not fit such data with non-interfering separate states, but do a full partial wave analysis. We hope to do this in the future.

Fig. 6 shows the ratio of data (1960/900).

While the ratio is consistent with being constant from threshold up to 1 GeV/c^2, it drops significantly in the mass region of the $f_2(1270)$. The lower ratio there is perhaps

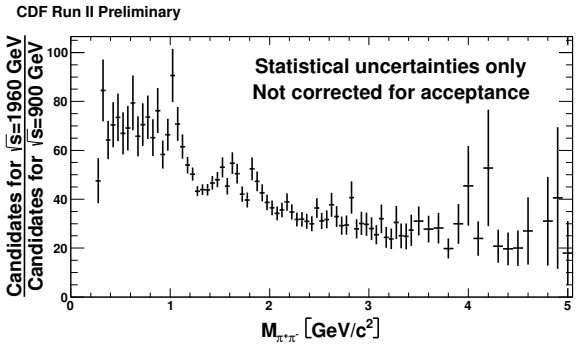

Figure 6: Ratio of mass distributions for $\sqrt{s} = 1960$ GeV and $\sqrt{s} = 900$ GeV

a spin effect. The downward trend of the ratio continues to above 4 GeV/c^2. The overall behavior of the $\sqrt{s}$ dependence as a function of mass gives a good benchmark to test models.

In the mass range 1.5 - 2.5 GeV/c^2 the data appear to show a wave structure. There are f_0 resonances here, but they are broad and/or not well established. The 900 GeV data do not have good enough statistics to verify this, and we do not have a good enough prediction of the shape of the distribution to test the significance.

6 Acceptance calculation

In order to present cross sections, such as $d\sigma/(dM.dp_T.dy)$ and unfold the acceptance $A(M, p_T, y)$ from the data, we calculate the acceptance, generating pion pairs and using CDFSIM to simulate the trigger and resonstruction efficiency. A parent state X is generated flat in rapidity with $-1.0 < y < +1.0$, in mass and p_T bins from 0 to 5.0 GeV/c^2, and 0 to 2.5 GeV/c respectively. In the absence of knowledge about spins and polarizations, X is made to decay isotropically (S-wave, J=0), and the final state particles are then specified.

All the forward off-line cuts were made (a decay particle could be forward, even if X was more central). The additional track cuts were simulated, and the acceptance $A(M, p_T)$ calculated as the ratio of generated to accepted events in bins of $M(X)$ and $p_T(X)$ weighted by trigger efficiency.

The trigger efficiency was determined data-driven by using well measured isolated tracks from minimum-bias data from same periods.

Finally, in order not to have fake structures from statistical fluctuations in the (finite!) Monte Carlo, we used a bilinear interpolation to compute the acceptance at every point. Fig. 7 shows $A(M, p_T)$ and the errors on it. We will not report cross sections for $M < 0.8$ GeV as the acceptance is low and strongly varying.

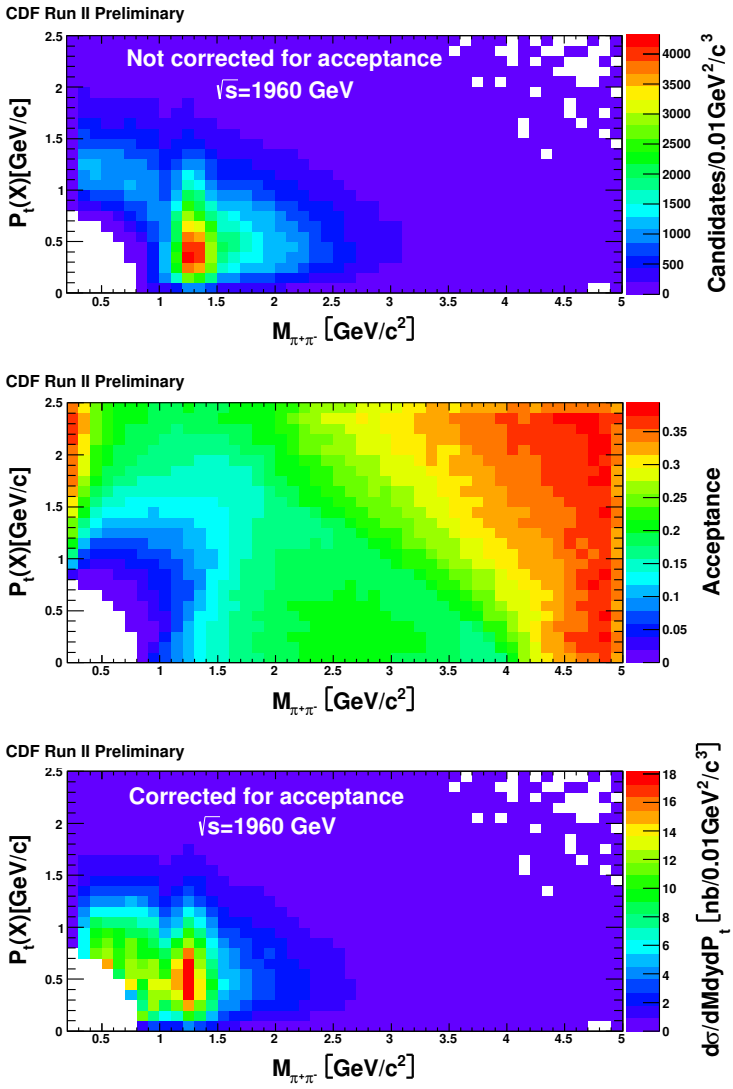

Figure 7: Top: $sqrts = 1960$GeV data before correction for acceptance. Middle: Acceptance as a function of invariant mass and p_T of central state, assuming isotropic (J=0, S-wave) decay to 2 charged pions. Bottom: $sqrts = 1960$GeV data after correction for acceptance

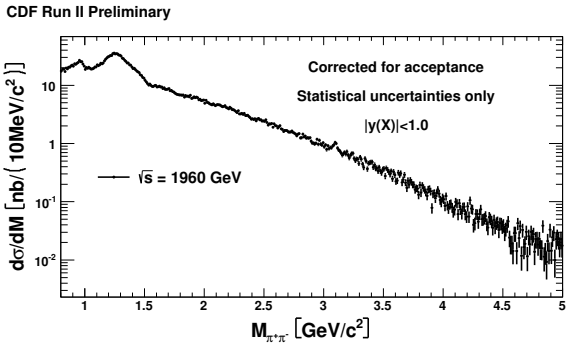

Figure 8: Invariant mass distribution of 2 particles assuming pion masses - corrected for acceptance in logarithmic scale. $\sqrt{s} = 1960GeV$

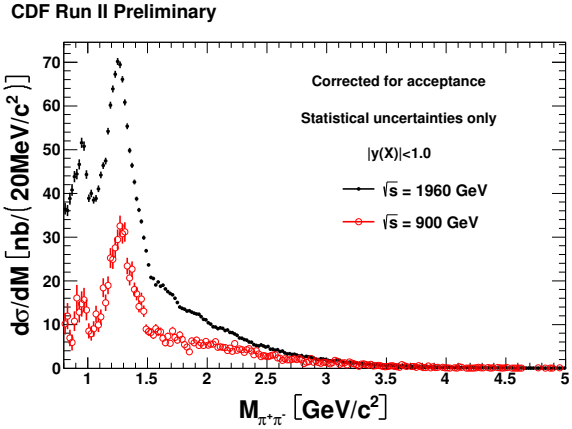

Figure 9: Comparison of invariant mass distribution of 2 particles assuming pion masses - corrected for acceptance, for two $\sqrt{s}$ energies, 1960GeV - black and 900GeV - red.

7 $\pi^+\pi^-$ cross sections

For each M, p_T (see Fig. 7) bin we divide the data by the acceptance to get the corrected mass distribution, and use the effective luminosity to get the cross section $d\sigma/dM$. The invariant mass plot integrated over all p_T range is shown in Figs. 8 and 9.

The mass spectrum shows many interesting structures.

7.1 Region $0.28 - 0.8GeV/c^2$

In this region, our kinematical requirements on the final state are such, that in low p_T region we have acceptance = 0, so we do not present integrated cross sections. On a not corrected for acceptance data plot (Fig. 10) we can see narrow structures comming from $\phi \to K^+K^-$ misidentified as pions, peak from $K0_S \to \pi^+\pi^-$, sign of non exclusive background and a $\rho(770)$ peak comming from photoproduction or again, non exclusive

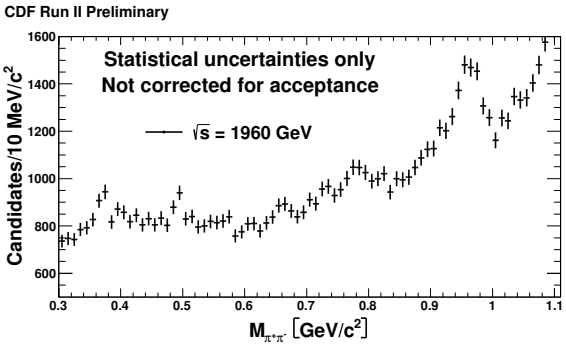

Figure 10: The invariant mass distribution in low mass region - not corrected for acceptance, $\sqrt{s} = 1960 GeV$

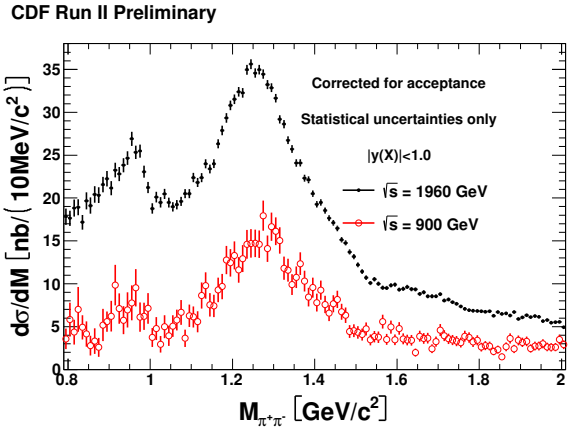

Figure 11: Comparison of invariant mass distribution of 2 particles assuming pion masses in low mass region - corrected for acceptance, for two $\sqrt{s}$ energies, 1960GeV - black and 900GeV - red.

background.

7.2 Region $0.8 - 2.0 GeV/c^2$

This region consists of the most clearly visible resonances on top of a continuum $\pi^+\pi^-$ structure, but one can not simply add background to signal, as they are both results of interference and scattering between the final state pions. We can clearly see the emergence of the $f_0(980)$ state, a sharp drop at the opening of K^+K^- threshold, then the biggest peak coming from (probably) the $f_2(1270)$ state. This peak shows structure that is not well approximated by single resonance (Breit-Wigner or Gaussian) but rather a sum of two. We suggest that this peak consists of interfering $f_2(1270)$ and broad $f_0(1370)$ states. Above this large peak, at 1.5 - 1.6 GeV/c^2, we see a clear and rapid change of slope. All these features are clearly visible for both energies in Fig. 11

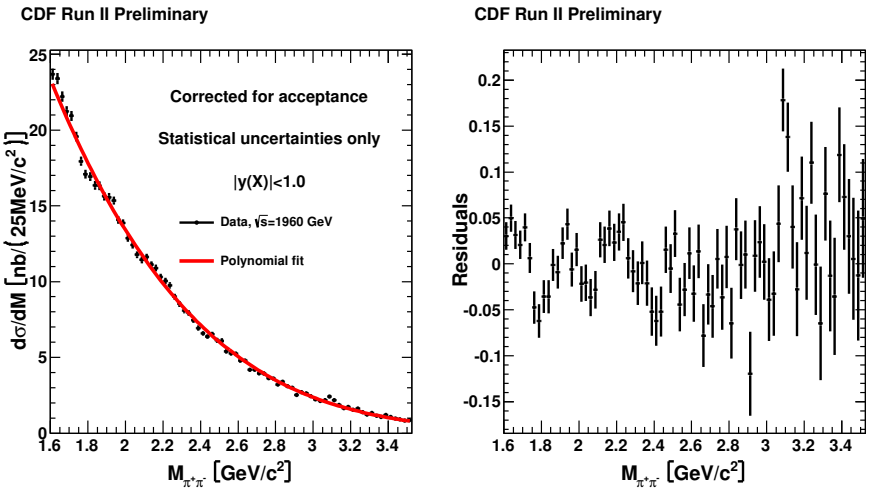

Figure 12: Left: Invariant mass distribution of 2 particles assuming pion masses - corrected for acceptance with 4'th order polynomial fit. Right: residuals of the left plot and fit. $\sqrt{s} = 1960GeV$

7.3 Region $1.6 - 5.0GeV/c^2$

The region above most prominent resonance shows bump structure, and is not consistent with simple curve. We believe that some broad f_0 states might be present there and interfere with continuum background. Our statistics are not high enough to resolve such states, but is enough to show the discrepancies from smooth fits. We tried to fit an 4th order polynomial (see Fig. 12) to this region, and we show the residuals.

7.4 Mean p_T

Another interesting kinematic variable is the p_T of central state. In Figs. 13 and 14 show the dependence of $\langle p_T \rangle$, corrected for acceptance, on the invariant mass. This distribution shows interesting structure and is remarkably independent of the $\sqrt{s}$ energy. A few of the distributions of p_T (for some of mass ranges at $\sqrt{s} = 1960GeV$) are shown in Figs. 15.

8 Search for χ_{c0}

The raw data plots Fig. 4 and Fig. 5 do not show a significant $\chi_{c0}(3415)$ signal both in $\chi_{c0} \to \pi^+\pi^-$ and $\chi_{c0} \to K^+K^-$, henceforth we set a 90% Bayesian upper limit for it's cross section. To do so, we estimate background under those possible resonances by fitting exponential distribution to our data points in mass range $[2.5 : 5.0]GeV/c^2$, excluding the regions where we could see excess comming from χ_{c0} or J/ψ with misidentified final particles. The fit is presented in Fig. 16.

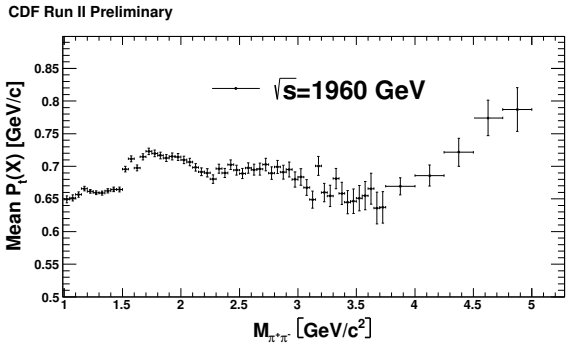

Figure 13: Mean value of the p_T distribution of central state decaying to two central pions as a function of invariant mass. $\sqrt{s} = 1960GeV$

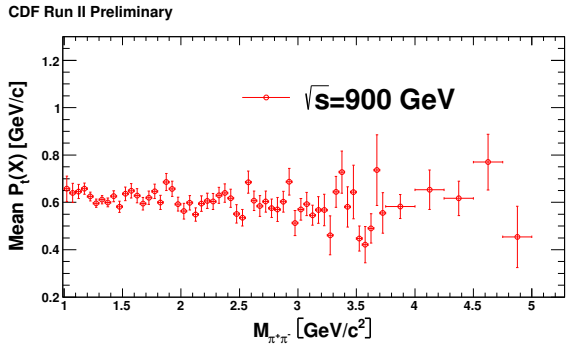

Figure 14: Mean value of the p_T distribution of central state decaying to two central pions as a function of invariant mass. $\sqrt{s} = 900GeV$

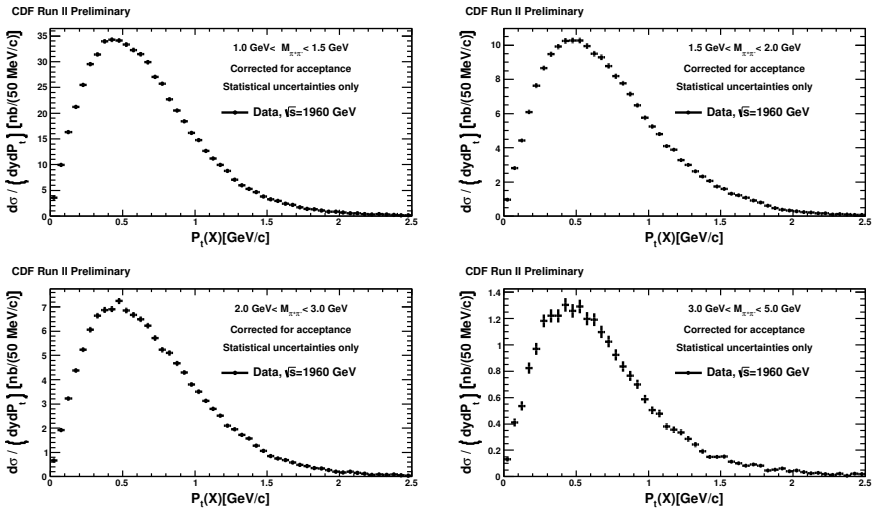

Figure 15: p_T distribution of central state decaying to two central pions in few mass windows. $\sqrt{s} = 1960GeV$

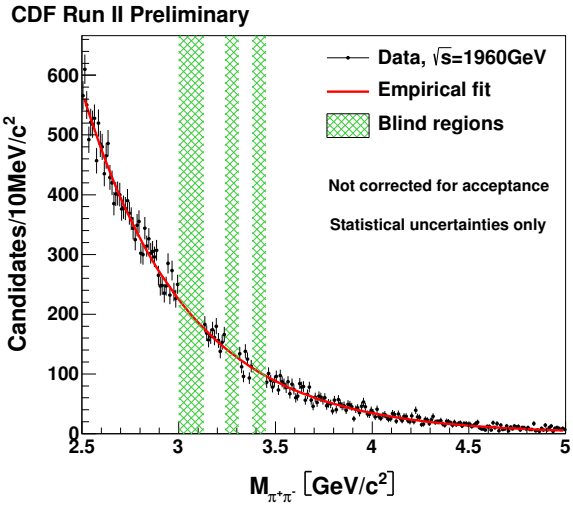

Figure 16: Invariant mass distribution of 2 particles assuming pion masses with exponential fit to region $[2.5 : 5.0]GeV/c^2$ excluding χ_c and J/ψ signal regions - corrected for acceptance. $\sqrt{s} = 1960GeV$

In $\chi_{c0} \to \pi^+\pi^-$ channel we set the 90% limit at 21.4 ± 4.3nb and in $\chi_{c0} \to K^+K^-$ channel we set it at 19.0 ± 3.8nb.

9 Future studies of $\pi^+\pi^-$ resonances

It should be possible to distinguish spin J = 0 and J = 2 states using decay angular distributions, or better a real partial wave analysis. In the AFS experiment this was done and could (a) observe a small P-wave (spin J = 1) signal at the $\rho(770)$, forbidden in DIPE, (b) show S-wave dominance up to 1 GeV with a J = 2 $f_2(1270)$ above that. In that experiment the forward protons were detected, providing additional information. In our data we have the 4-vector of X, and can study the decay angular distribution with respect to that direction.

9.1 K^+K^- background in $\pi^+\pi^-$ data.

An estimate of size of K^+K^- background in $\pi^+\pi^-$ sample is given by the pairs identified by dE/dx as K^+K^-. This can only be done in when both hadrons have momenta in the range 400 MeV/c (our cut) up to 750 MeV/c.

This study shows that (assuming independence of π/K production ratio of momentum) the K^+K^- background in our $M(\pi^+\pi^-)$ spectra is approximately 12%.

The beter estimate is to be expected by future measurement of $K0_SK0_S$ production cross section and invariant mass distribution in $DIPE$.

10 Summary and Conclusions

This is a work in progress. For now (August 2012) we have shown a large sample of exclusive h^+h^- events (much larger than in other experiments), mostly $\pi^+\pi^-$, that show several resonance features. The further background rejection on basis of COT and SVX information is being studied, as well as other possible kinematical cuts for different states S/B enhancments. The partial wave analysis for this data is one of most important updates. Other channels are being studied.

References

[1] Quantum Chromodynamics and the Pomeron, J.R.Forshaw and D.A.Ross, Cambridge Lecure Notes in Physics, Cambridge University Press, 1997.

[2] V.Barone and E.Predazzi, High Energy Particke Diffraction, Springer, 2002.

[3] S.Donnachie, G.Dosch, P.Landshoff and O.Nachtmann, Pomeron Physics and QCD, Cambridge University Press, 2002.

[4] M.G.Albrow, T.D.Coughlin, and J.R.Forshaw, Central exclusive particle production at hadron colliders, Prog.Part.Nucl.Phys. **65**, 149 (2010).

[5] J.L.Rosner, Phys. Rev. D **74** 076006 (2006).